13

Corrosion Monitoring of the Steam Generators of V-th and VI-th Energy Blocks of Nuclear Power Plant "Kozloduy"

Nikolai Boshkov, Georgi Raichevski, Katja Minkova and Penjo Penev
Institute of Physical Chemistry, Bulgarian Academy of Sciences
Nuclear Power Plant "Kozloduy"
Bulgaria

1. Introduction

Corrosion resistance and erosion wear of the metal equipment (body, pipe bundles, steam generators etc.) are of great importance for the operating time limit of the nuclear power plants (NPP) bearing in mind their extremely heavy technological and water-chemical regime (WCR). The horizontally placed steam generators (SGs) used in the Energy Blocks of NPP "Kozloduy" work at exploitation conditions leading to corrosion and erosion provoked processes (Andreeva M. et. al., 2008). Similar is the situation in the greater part of the modern power plants (R.W. Staehle & J.A. Gorman, 2003; R.W. Staehle & J.A. Gorman, 2004; R.W. Staehle & J.A. Gorman, 2004). This fact predetermines the necessity of very careful daily and also periodical monitoring concerning the real operating state of the equipment during its exploitation time (Sviridenko, I., 2008; Hadavi, S.M.H., 2008; Viehrig, H.-W., et. al., 2006; Slugen, V., et. al., 2005). The evaluation and explanation of the obtained results for the electrochemical-corrosion parameters will ensure a realistic base for a precise prognosis and trouble-free operation of the installations (J. Congleton et all, 1985; Raichevski G. et al.,. 2007; Hojna A. et. al, 2007; Kaczorowski D. et. al., 2006).

Markedly dangerous negative influences leading to technical failures and damages have the conglomerated corrosion products (CPs) the latter appearing as a result of the WCR mainly in the second contour of NPP. Considerable part of them enters the condense-feeding part of SGs and deposit as loose layers on the pipe surface or falls as middling slime on the bottom changing in such a way the overall electrochemical and hydrodynamic situation in the internal volume during the operation procedures.

In general, CPs presenting in the steam generators consist of iron and copper oxides and hydroxides. If their adhesion to the surface is enough strong (for example, like in the case of magnetite – Fe_3O_4) it can be expected that a passive layer will appear on the surface of the equipment and in such a way this part of the installation will be additionally protected. If CPs are crumbly the operative situation in the SGs will be worsen since these deposits often lead to accelerated formation and development of local corrosion phenomena – holes, pits, cracks, including appearance of stress corrosion cracking process etc., the latter being one of the most dangerous events due to its practical invisibility up to the moment of the sudden physical-mechanical destroying (Zubchenko, A.S., et al., 2004; Slugen, V., et al., 2002; Lunin, G.L., et al., 1997; N.D. Budiansky, et al., 2005).

The presence of sulphate, copper and especially chloride ions additionally contributes to the corrosion damages resulting in local ruptures with different sizes. When CPs have loose structure and high porosity the concentration of Cl^- ions in their volume increases due to the flowing capillary processes. This effect is stronger expressed in the contact places of the pipes with the distance grid as well as at the lowest placed rows of the pipe bundles in SGs.
In general, the aim of the present investigation is to determine and evaluate the role of different aggressive components presenting in the technological medium on the corrosion behavior of austenitic stainless steel of the type 18Cr10NiTi which material is used to produce the pipe bundles in the SGs of the second contour of Energy blocks No. V and No. VI of NPP "Kozloduy". Some of the results obtained by polarization technique are compared with the experimental data of low-alloyed steel.

2. Experimental

2.1 Samples

Two different steel sample types with dimensions 1 x 1 cm (working area of 2 cm^2) are used:

- High-alloyed (HAS) austenitic stainless steel 18Cr10NiTi which is applied as a main construction material for the pipe bundles in the SGs of NPP "Kozloduy" (composition: Cr – 18 wt.%; Ni – 10 wt.%; Ti – about 1 wt.%; balance – Fe).
- Low-alloyed (LAS) steel 38GN2MFA (composition: Cr, Ni, Mn and Si – about 6 wt.% total; balance - Fe) used in general as a construction steel and as a comparative sample.

2.2 Corrosion medium

The corrosion tests are carried out in a model corrosion medium (MCM) consisting of trebly distilled demineralised water (specific electric conductivity ≤ 1 μS/cm), hydrazine (25 μg/L) and in definite cases selected anions or cations (Cl^-, SO_4^{2-}, Na^+, Cu^+, Cu^{2+} - both latter presented in the text as Cu_{total}). The pH value is about 9 aiming the modelling of conditions maximal close to the exploitation ones. Special attention is paid to the effectiveness of the added compound that inhibits the development of the damaging processes on the surface and in the depth – monoethanolamine (MEA) at concentration of 2 mg/L.

2.3 Sample characterization

2.3.1 Potentiodynamic (PD) and potentiostatic (PS) polarization curves

Potentiodynamic (PD) polarization curves (scan rate of 1 mV/s.) are carried out at two selected operating temperatures (35 °C and 95 °C, respectively) in a three-electrode experimental glass cell using "VersaStat" (AMETEK PAR) device. The cell has a volume of 300 cm^3 and Luggin capillary for minimizing the Ohmic resistance. Platinum plate serves as a counter electrode and saturated calomel electrode (SCE) - as a reference electrode.
The investigations of the local corrosion phenomena are realized in a special constructed test electrode the latter allowing simulation of the processes taking place in cracks with different widths. This electrode consists of ceramic body, separators (mica lamellas), titanium linings etc. giving the opportunity to work also at high temperatures and pressures aiming the modelling (approaching) of the real operating conditions in the SGs.
In order to receive also several results at conditions maximal close to the exploitation ones an autoclave system is used for some of the electrochemical and corrosion measurements. The autoclave volume is approximately 1,5L and its maximum capacity is to work at temperatures of 350 °C and pressures of 150 atm. Aiming better safety the experiments are

carried out in the interval of about 220 - 230 ^{o}C and pressure of 150 atm. Three-electrode electrochemical Teflon cell with working volume of 300 cm^3 and Ag/AgCl reference electrode assembly is mounted in the autoclave unit. The polarization studies in that case are carried out in a potentiostatic way contrary to the anodic and cathodic polarization curves realized at the abovementioned temperatures and at atmospheric pressure.

2.3.2 Scanning electron microscopy

SEM images and EDX analysis complete the results of the investigation giving more information about the surface morphology of the tested samples and of the collected CPs. A scanning electron microscope JEOL JSM-5300, Japan (equipped with EDX device) is used for registration of the morphology changes on the sample surfaces of HAS after the treatment in the medium. This device is used also for quantitative analysis of the element composition in selected special places – pits, cracks etc. The results obtained by this method ensure the possibility to present more realistic prognosis about the future exploitation of the SGs.

2.3.3 Moessbauer spectroscopy

Moessbauer spectroscopy completes phase analysis of the chemical compounds for characterization of the type and quantity of the iron compounds presenting on the sample. This method is based on the high sensitivity of Fe in relation to the resonance adsorption toward the beams of the radiation source applied. In the present investigations the absorption variant of the method is used which allows to receive information from the whole thickness of the CPs. The separation of the phases is realized with high sensitivity accepting that the whole amount of all compounds presenting is 100%. Actually, Moessbayer spectra are carried out at room temperature using electromechanical spectrometer working at conditions of a constant acceleration with a ^{57}Co/Cr source (activity ≅ 60 mCi) and α-Fe probe as a standard. Experimentally obtained spectrum is additionally calculated using a special program based on the method of the least squares. The content of iron ions in every component is determined under the conditions of the presumption of identical Moessbayer-Lamb factor.

2.3.4 X-ray photoelectron spectroscopy

XPS analysis is carried out with ESCALAB MkII (VG Scientific) electron spectrometer characterizing with base pressure in the chamber up to 5 x 10^{-10} mbar (during the test 1 x 10^{-8} mbar) with MgKα X-ray source (excitation energy hν = 1253,6 eV).
Due to the weak signals for Ni2p and Cr2p as well as the presence of a broadly expressed Fe2p line an accelerating energy value of 50 eV and a sighthole with 6 mm width (entry/exit) is used. Instrumental resolution measured as full width at a half maximum (FWHM) of the photo electron peak of $Ag3d_{5/2}$ is lower than 1 eV. The binding energy scale is corrected to the maximal C1s peak at 285 eV for electrostatic charge. The spectra obtained are additionally analyzed using symmetric fitting Gauss-Lorenz curve after eliminating the background accordingly to the requirements of the method of Shirley.

3. Results and discussion

3.1 Potentiodynamic polarization investigations

3.1.1 Potentiodynamic investigations of low-alloyed steel (LAS)

The results for the corrosion behavior of LAS at 35 ^{o}C are demonstrated in Figure 1 and are used to characterize this steel and as a benchmark for comparison with high-alloyed steel.

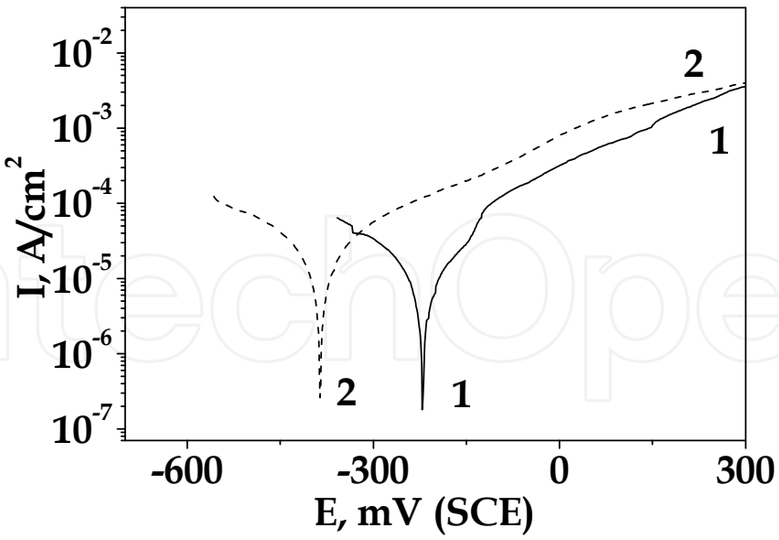

Fig. 1. PD polarization curves of LAS at 35 °C in:
1 – MCM; 2 – MCM with addition of 10 μg/L Cl^-.

It can be registered that even at low concentration of the added corrosion activators - Cl^- ions (10 μg/L), curve 2 - their unfavourable influence is well expressed. As seen from the results the corrosion potential value (E_{corr}) of the tested steel sample is strongly shifted in negative direction in that case with about 170 mV compared to the same parameter in the initial MCM (curve 1). Accordingly to this observation and as could be expected, the corrosion current density (i_{corr}) and the rate of the active anodic dissolution in the presence of chloride ions are about 2-3 times higher leading to accelerated damaging processes (greater anodic dissolution) under the conditions of external polarization.

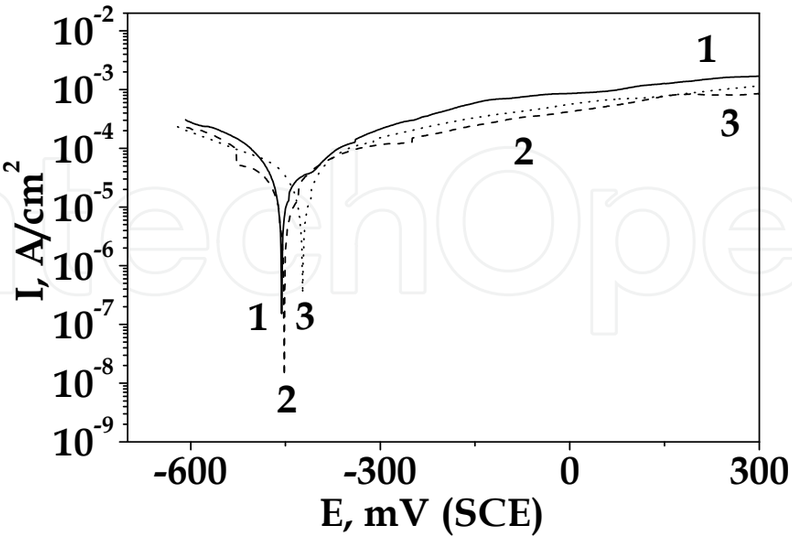

Fig. 2. PD polarization curves of LAS at 35 °C in:
1 – MCM with 300 μg/L Cl^-; 2 – MCM with 300 μg/L Cl^- and 2 mg/L MEA;
3 – MCM with 1 mg/L Cl^- and 2 mg/L MEA.

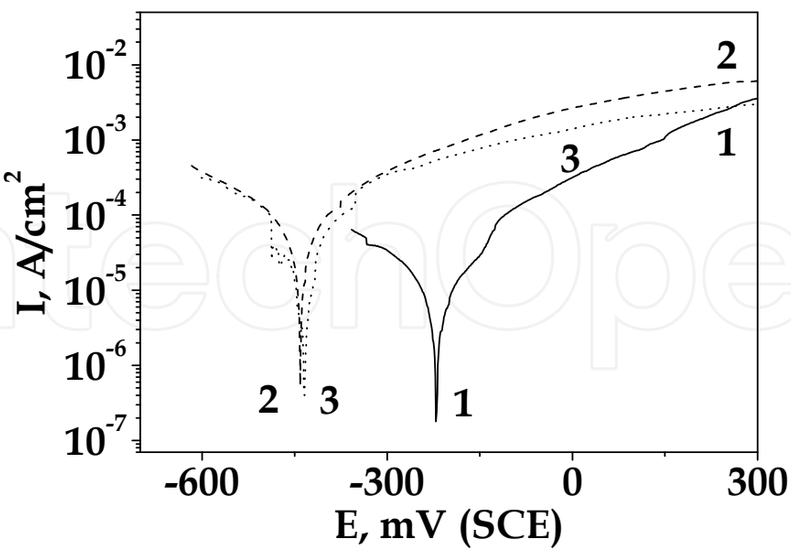

Fig. 3. PD polarization curves of LAS at 35 °C in:
1 – MCM; 2 – MCM with 300 µg/L SO_4^{2-};
3 – MCM with 300 µg/L SO_4^{2-} and 2 mg/L MEA.

Further increasing of the Cl^- ions concentration up to 300 µg/L (Figure 2, curve 1) results in another potential shift in the negative direction with about 200 - 230 mV compared to the case in MCM without addition of activators (Figure 1, curve 1) and with about 70 mV compared to case with the lower Cl- concentration (Figure 1, curve 2). Corrosion current density value also increases especially in the potential range between -300 and 0 mV (SCE). The addition of MEA even at not very high concentration (that could be applied in the practice) plays definitely a positive role – curve 2 – leading to lower corrosion and anodic current density values and fixing the further shifting of the corrosion potential. Even at very high concentration of corrosion activators (1 mg/L chloride ions – Figure 2, curve 3) the presence of the added corrosion inhibitor MEA decrease partially the cathodic (oxygen reduction) and also the anodic (metal dissolution) reactions demonstrating lower corrosion current - i_{corr} – values and ensuring better protection against corrosion.
Similar effect of MEA is observed also in the case when sulphate ions are used as corrosion activators in the same model medium and at the same experimental conditions (Fig. 3). The corrosion potential is shifted with about 220-230 mV in negative direction (curve 2) and i_{corr} increases about 4 – 5 times. After the addition of MEA the anodic dissolution rate is slowed down (curve 3) which demonstrates the positive influence of this compound. That result leads also to the conclusion that the protecting mechanism of MEA is most probably similar in aggressive media with different corrosion activators.
It is very important for the practice to register and estimate the effects also in the case when some of the most dangerous corrosion activators (Cl^-, SO_4^{2-} and Cu_{total}) simultaneously present in the medium at their extreme high concentrations.
The results obtained for LAS treated in this type of model solution are demonstrated in Fig. 4. It is evident that E_{corr} is strongly shifted in negative direction again and the corrosion current density values are very high which can be expected at these conditions. Also at these

extremely aggressive medium the addition of MEA decreases the i_{corr} and the dissolution in the whole anodic region. The reason for this positive result is that the influence of MEA simultaneously slow down the cathodic (reduction of depolarizer) and the anodic (dissolution of the metal) reaction rates. It can be supposed from these observations that the used compound MEA is an inhibitor of a "mixed" type.

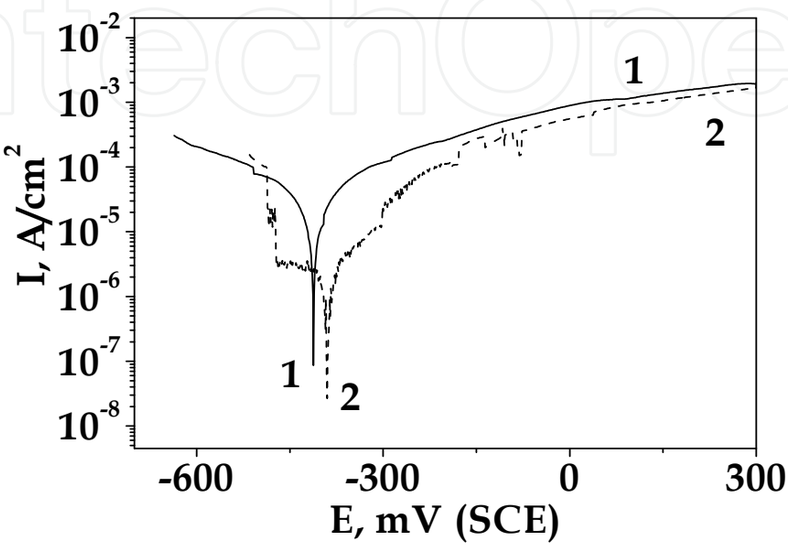

Fig. 4. PD polarization curves of LAS at 35 °C in:
1 – MCM with 1 mg/L Cl^-, 1 mg/L SO_4^{2-} and 5 µg/L Cu_{total};
2 – MCM with 1 mg/L Cl^-, 1 mg/L SO_4^{2-}, 5 µg/L Cu_{total} and 2 mg/L MEA.

The potentiostatic studies in the autoclave realized in MCM containing chloride ions show a slight shift of the corrosion potential in cathodic direction and about 3,5 times increase of the corrosion current density value for this steel type.

3.1.2 Potentiodynamic investigations of high-alloyed steel (HAS)

The results obtained for HAS which is practically used in the steam generators are demonstrated in Figure 5. It can be observed that low Cl^- ions concentration in the model medium (10 µg/L) – curve 2 - increases significantly (about 4-5 times) the corrosion rate. Additionally, well expressed shift of E_{corr} in negative direction of about 300 mV can be registered. Nevertheless, compared to the case of LAS (see Figures 1 and 3, curves 1) i_{corr} is about 5 – 6 times lower at these conditions. The registered differences are attributed to the better protective influence of the alloying components presenting in HAS. The addition of MEA (curve 3) expresses strong favourable effect leading to the shifting of E_{corr} in positive direction with about 350 mV while i_{corr} decreases about 4 times compared to the case of MCM with addition of Cl^-, but without MEA (compare curves 2 and 3).
Similar is the influence of MEA also in the case when SO_4^{2-} ions present as activators at equal concentrations in the model medium (Figure 6). As can be registered sulphate ions extremely increase the corrosion current density but the addition of MEA leads to inhibiting of the corrosion and anodic processes.

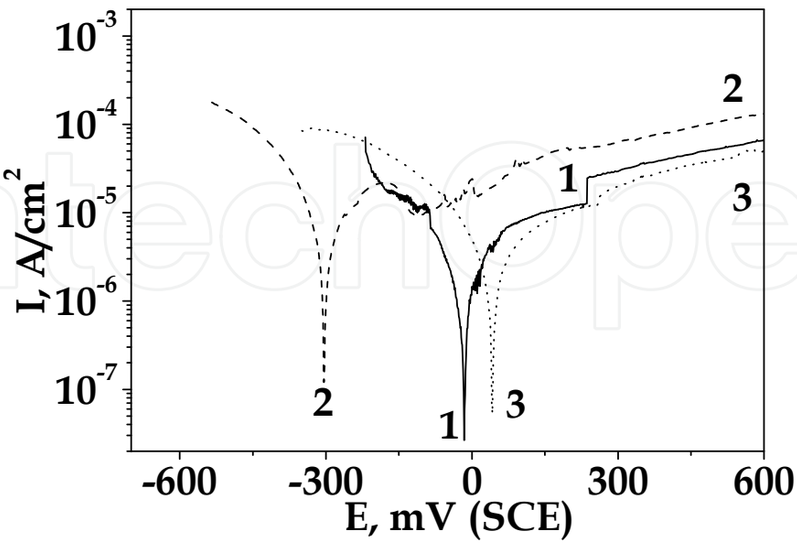

Fig. 5. PD polarization curves of HAS at 35 °C in:
1 – MCM; 2 – MCM with 10 μg/L Cl^-;
3 – MCM with 10 μg/L Cl^- and 2 mg/L MEA.

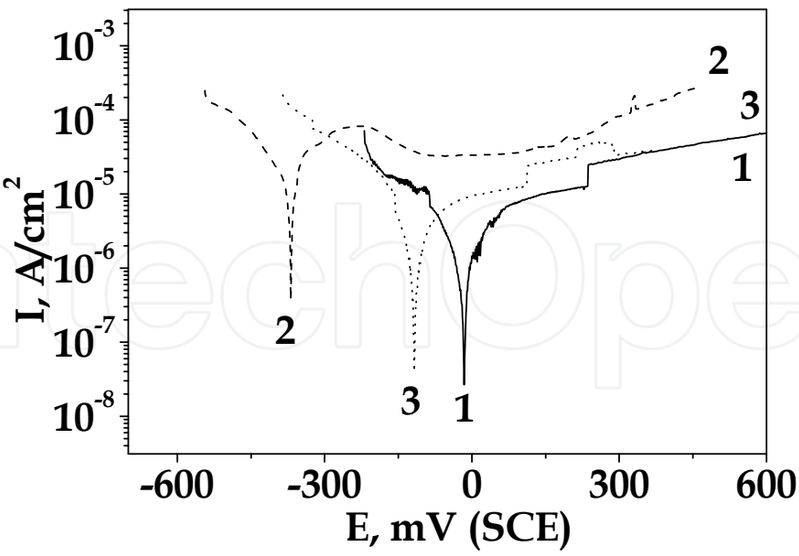

Fig. 6. PD polarization curves of HAS at 35 °C in:
1 – MCM; 2 – MCM with 300 μg/L SO_4^{2-};
3 – MCM with 300 μg/L SO_4^{2-} and 2 mg/L MEA.

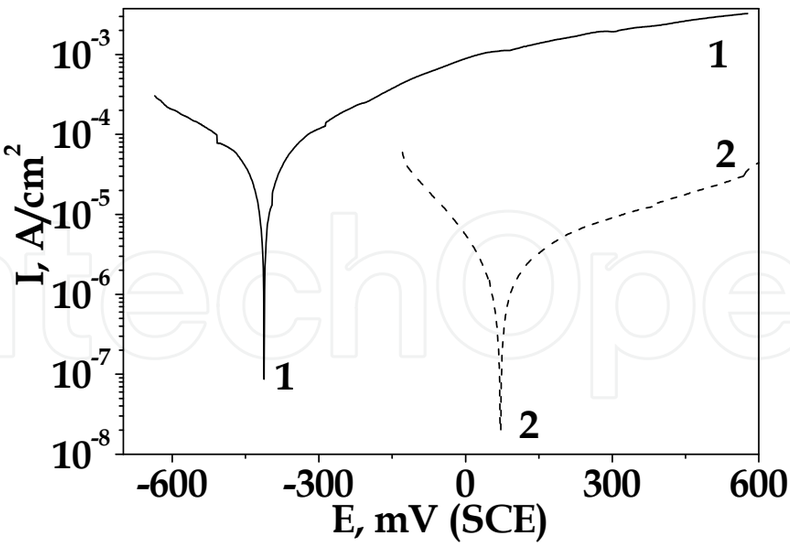

Fig. 7. PD polarization curves of HAS at 35 °C in:
1 – MCM with 1 mg/L Cl^-, 1 mg/L SO_4^{2-} and 5 µg/L Cu_{total};
2 – MCM with 1 mg/L Cl^-, 1 mg/L SO_4^{2-}, 5 µg/L Cu_{total} and 2 mg/L MEA.

In the case, when the combination of the most dangerous activators (Cl^-, SO_4^{2-} and Cu_{total}) is applied in MCM the corrosion activity is also very strong demonstrated - Figure 7. It is evident from the figure that the corrosion rate in that case is much greater and the corrosion potential is additionally shifted to the negative direction up to the value of about -410 mV.
Nevertheless, the inhibiting effect of MEA is also very strong (curve 2) - the corrosion potential is placed in positive direction, i_{corr} value is more than 10 times lower and the anodic dissolution seems to be partially hampered. The latter can be explained with the process of the effective inhibitor adsorption exactly on the active anodic zones on the metal surface. Finally, it could be prognosticated that MEA will slow down the corrosion processes also at exploitation conditions in the case when the three activators simultaneously present in their extreme high for the practice concentrations.
The potentiostatic investigations in the autoclave show more clearly expressed shift of the corrosion potential in cathodic direction with about 100 mV and about 4 times increase of the corrosion current density value for this steel. Despite of these results the new data obtained from this test are much lower compared to the case of LAS.

3.1.3 Potentiodynamic investigations of HAS in cracks

As a result of the operating conditions and WCR the equipment in NPP and in particular the SGs can be effective damaged by large number of cracks, holes, slits etc. This is a specific type of local corrosion and these dangerous places strongly differ in their morphology and element content compared to the whole surface of the unit. For example, in the case of newly appeared cracks the electrochemical potentials in and outside can be extremely different which will lead to appearance of galvanic macro-elements with own electromotive force. It is very important to know that local corrosion phenomena can appear not only in the already existing constructive slits. During the exploitation new cracks can occur especially in the cases where different materials or media are in contact or as a result of simultaneous action of electrochemical and mechanical forces.

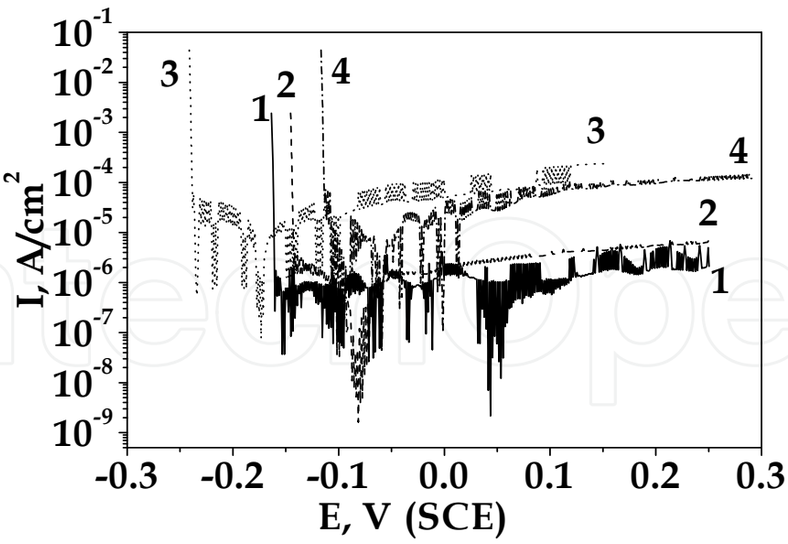

Fig. 8. PD curves of HAS in MCM with 1 mg/L Cl^-, 1 mg/L SO_4^{2-} and 5 µg/L Cu_{total}:
1 – in crack 0,5 mm at 35 °C; 3 - in crack 0,1 mm at 35 °C;
2 - in crack 0,5 mm at 95 °C; 4 - in crack 0,1 mm at 95 °C.

It such a case it is very important to know the current density value into the crack that can be mould out of a specially constructed for this case electrode. It allows simulating the corrosion processes in cracks with different preliminary fixed widths. The present investigations are realized using two artificially constructed widths (sizes of 0,1 and 0,5 mm respectively). For practical purpose the special electrode has being filled in with the experimental solutions (with or without addition of corrosion activators) directly before the beginning of the test aimed to eliminate possible diffusion limitations.

The polarization investigations presented here (Fig. 8 and Fig. 9) are carried out in MCM containing the extreme high concentrations of the corrosion activators – 1 mg/l Cl^-, 1 mg/l SO_4^{2-} and 5 µg/l Cu_{total} – with and without addition of MEA, respectively. Comparing the characteristic parameter E_{corr} following can be summarized – Fig. 8:

- at 35 °C E_{corr} for the narrower crack (0,1 mm – curve 3) is strongly replaced in negative direction with about 100 mV compared to the wider one (0,5 mm - curve 1) as a result of the reasons described above;
- at 95 °C E_{corr} of both samples are relative closer – compare curves 2 and 4.

The oscillations of the curves are most probably on account of the inhibition of the processes of access and taking away the oxygen into the depth of the crack. In the anodic region the current density values are higher in the case of the narrower crack which means that the processes of dissolution are strongly expressed.

The addition of MEA in concentration of 2 mg/l shows favourable effect – E_{corr} shifts in positive direction for all investigated samples (compare Figures 8 and 9). Additionally, the observed i_{corr} values are also lower at both temperatures and crack widths – Fig. 9 – which is a sign for inhibiting of the corrosion processes. The electrochemical behavior of the steel in the narrow cracks and holes characterizes with some peculiarities mainly as a result of the transportation difficulties – inhibited access of the corrosive and passivating agents and difficult take away of CPs from these places. In neutral medium Fe shows increased rate of the anodic process and decreased – of the cathodic one. The lower oxygen concentration in

the cracks leads to more negative potentials of iron ionization with predominantly formation of bi-valence ions and their compounds the latter in general possessing insufficient protective properties.

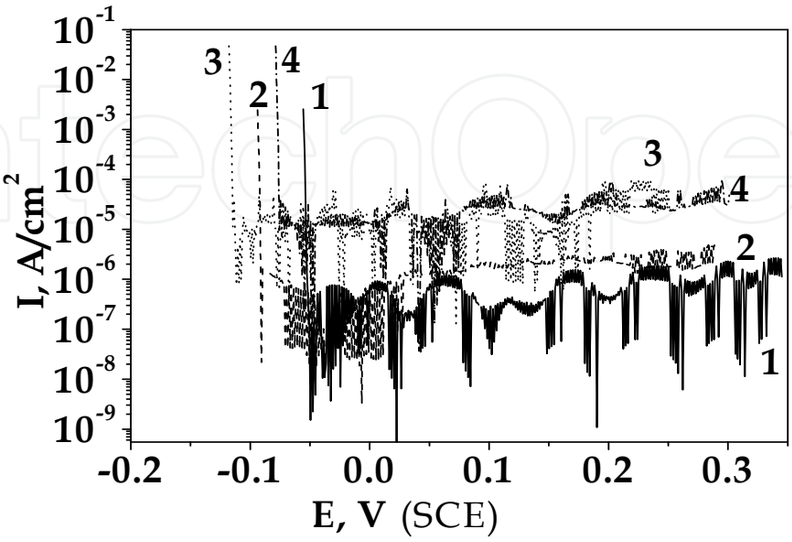

Fig. 9. PD curves of HAS in MCM with 1 mg/L Cl^-, 1 mg/L SO_4^{2-}, 5 μg/L Cu_{total} and 2 mg/L MEA:
1 – in crack 0,5 mm at 35 °C; 3 - in crack 0,1 mm at 35 °C;
2 - in crack 0,5 mm at 95 °C; 4 - in crack 0,1 mm at 95 °C.

The passive state of the metals owed mainly to the presence of oxygen may be affected by inhibited access of this component leading to depassivating and accelerating of the anodic reaction. Additionally, the cathodic reduction of the depolarizer becomes slowly, E_{corr} and PD curves shift to negative direction. The reason for this effect is the fact that the electrolyte situated in the cracks does not intermix convectively any more and the oxygen transportation occurs only by molecular diffusion. The inhibited refreshing of the electrolyte leads to relative fast change of the pH value of the medium in these places compared to the surface outside the cracks. The composition of the electrolyte in these close volumes also changes during the exploitation process and as result oxides, hydroxides etc. accumulate on the surface. Their concentration depends in general on the product of solubility value of the CPs. The main changes of the corrosion medium in the cracks appear as a result of the macro-element activity between these places and the "bare surface". The metal inside the cracks works as an anode and after incubation period during which the current of the galvanic element is very low the "inner" electrolyte becomes more acidic that leads to beginning of depassivation process.
After prolonged exploitation of the equipment the corrosion damages in the cracks become extremely dangerous due to the fact that the appearance of the passive state of the steels is ensured mainly from the oxygen in the medium. The permanent lack of this element into the deep volume of the cracks leads to depassivating of different places and acceleration of local corrosion processes. These results confirm that the modelling (although approximately) of the exploitation conditions is useful and necessary in order to receive experimental data for dangerous corrosion phenomena and their detrimental influence as well as to give the opportunity to prognosticate them.

3.2 SEM and EDX investigations

3.2.1 SEM investigations

Steel samples are initially placed in the special electrode for investigation of the corrosion processes in cracks with different widths. Thereafter the same electrode is putted in an autoclave and leaved at E_{corr} in MCM containing the extreme high concentrations of chloride, sulphate and copper ions. One 24 hours-cycle test consists of 4 hours stay at the operating conditions (selected temperature and pressure) followed by 20 hours for equalizing with the room temperature (slow cooling process). The SEM images of HAS samples are presented in Fig. 10(A,B). The results are obtained after preliminary preparation of the corrosion treated steel samples – rinsing with distilled water and drying with hot air.
Figure 10A shows typical corrosion damages of HAS samples placed in the electrode with 0,5 mm width after 3 cycles of the corrosion treatment described above. It can be registered that after the treatment a damaged place appears on the surface. Much hardly attacked seems to be the sample simulating the crack with 0,1 mm width – Fig. 10B. The reasons for this result are most probably the lower oxygen concentration in the solution. Additional risk is the accumulation of loose corrosion products in which mass the activators concentration will be greater.

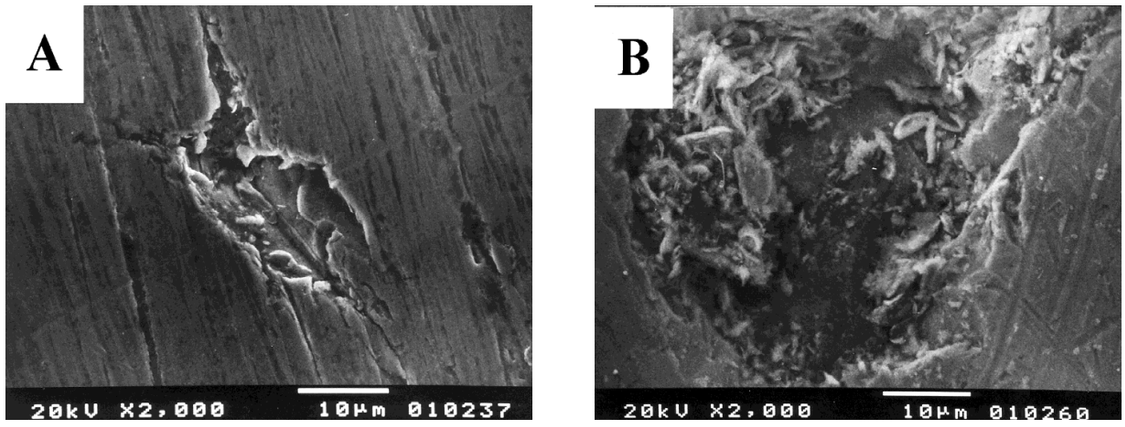

Fig. 10. SEM images of steel morphology after corrosion treatment of HAS samples:
A – in simulated crack with 0,5 mm width; B – in simulated crack with 0,1 mm width.

3.2.2 EDX investigations

The method gives the opportunity to determine the element composition in selected places on the steel surface characterized with different phenomena and processes - local holes, cracks etc. appeared after ruptures of the passive film. It is well known that after a definite time period the passive film in or over the crack or pitting can be totally destroyed and as a result open pits take shape. The average results from the analysis inside selected separate pits registered on the surface of the sample placed in the special electrode for investigation of the corrosion processes in the cracks and tested in MCM are presented in Table 1.
The main differences in the composition of the pits registered with and without MEA refer to the alloying components – Cr and Ni – both latter demonstrating higher percentages in the case with MEA. This is a clear positive effect since higher Ni and Cr amounts inhibit the penetration of the corrosion processes into the depth. The higher amount of iron detected when MEA present in MCM means that the dissolution of this metal is slowly.

Element	Content (in wt.%) after treatment in MCM	
	without MEA	with MEA
Fe	63,6	66,3
Cr	15,7	18,7
C	9,9	3,8
Ni	8,5	10,0
Si	1,9	0,8
Ti	0,4	0,4

Table 1. EDX analysis in selected pits and influence of MEA

3.2.3 SEM investigations of CPs

As already presented above the presence of MEA in the exploitation (or model) medium plays a positive role concerning the corrosion processes leading to their inhibiting. This compound can influence the appearance and development of the corrosion damages especially in places with limited oxygen access. The looseness, adhesion and the average size of the CPs particles are also of great importance in that case.

In the steam generators the corrosion products deposit on the body, pipe bundles, distance grids, bottom etc. and have in general sizes between 1 and 10 μm. On some places a compact film with good adhesion and low solubility consisting mainly of magnetite (Fe_3O_4) can appear. Additionally, a loose mass of new porous and with bad adhesion layers accumulate on it. As a result a strong increase of the local concentrations of Cl^-, SO_4^{2-} and Cu_{total} ions occur which leads to depassivation and appearance of pits on several places. In that sense some changes in the WCR leading to CPs with high dispersion are desirable aiming the easier removing of the particles from that zones.

The addition of MEA results in obtaining of CPs with high dispersion having average particle sizes less than 1 μm. Positive sign is also the fact that MEA do not lead to changes in the element and phase composition of CP. These effects are presented in Fig. 11.

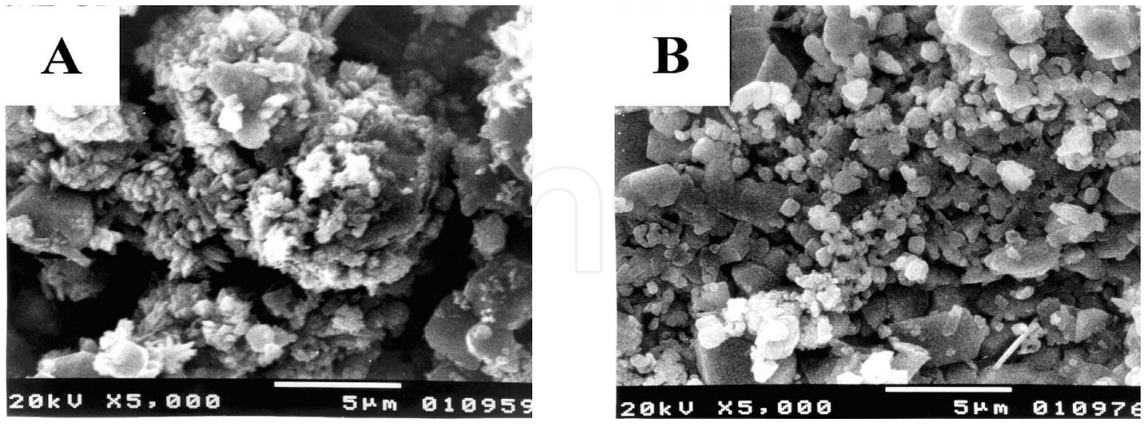

Fig. 11. SEM images of corrosion products:
A – without MEA in the medium; B – in the presence of 2 mg/l MEA.

3.3 Moessbauer investigations

The Moessbauer analysis (Fig. 12) of the surface film of corrosion products collected from characteristic places from the inner volume of the SGs during the shut-down procedure

show that the film consists of magnetite - Fe_3O_4 - and alpha-hematite - α – Fe_2O_3. As well known, these compounds are low soluble and highly resistive oxides, even in aggressive corrosion medium. This fact suggests that the corrosion products on the bundle surfaces may form a layer with high protective properties the latter impeding the penetration of the destructive corrosion processes in the depth of the metal tubes. The obtained average results are presented in Table 2.

Components	Weight %
Sxt 1 - Hematite, α – Fe_2O_3	62
Sxt 2 - Magnetite – tetra, Fe_3O_4	15
Sxt 3 - Magnetite - octa, Fe_3O_4	23

Table 2. Results from Moessbauer investigations

The experimental Moessbauer spectra include two types of components:
- components without super fine magnetic structure – quadruple doublets
- components with expressed super fine magnetic structure – sextets

In the present case the models for computer calculating of the Moessbauer spectra include only sextets (three sextet components). The values of the determined parameters of the six-component lines in the spectra (marked as Sxt 1, Sxt 2 and Sxt 3 in Table 2) can be attributed to the presence of iron-oxide phases – α–hematite (Sxt 1) and magnetite (Sxt 2 and Sxt 3). These two phases characterize with well expressed super fine magnetic structure (sextet components).

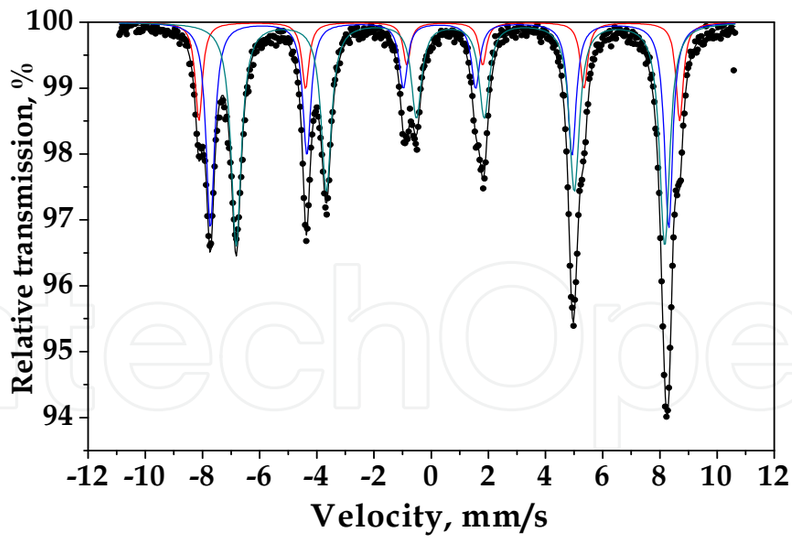

Fig. 12. Moessbauer spectra of CPs taken from SGs (average results)

The registered parameters for Sxt 1 demonstrate that all iron ions exist in the third oxidized state and octahedral surrounding. The appearance of two components of the magnetic phase, Sxt 2 and Sxt 3, is due to the existence of Fe in the third oxidized state and in tetrahedral surrounding. This is the reason for the presence of Sxt 2 in the spectrum as well as to a spectral appearance of iron ions with interstitial oxidized state ($Fe^{2.5+}$) in octahedral

position (its spectral expression is Sxt 3). As well known, magnetite is one of the widely distributed mixed valence compound with high frequency electron exchange between the ions $3d^6Fe^{2+} \leftrightarrow 3d^5Fe^{3+}$. Magnetite characterizes with cubic symmetry and the results demonstrate that it is with low degree of non-stoichiometry - Fe_3O_{4-x}, while the vacancies are localized most probably in the octahedral places.

3.4 XPS investigations

The results described below are related to powder CPs selected from different places in the volume of the SGs during the shut-down procedure. The data presented in Table 3 are summarized for all test samples.

Element	O 1s	Fe 2p	Cu 2p	Cr 2p	Ni 2p
Binding energy, eV (main peaks)	529,9 531,2	711,1	932,9 934,5	576,8	855,2
Percentage, at.%	76	8	14	1	1

Table 3. Results from XPS investigations of CPs taken from the inner volume of SGs (average results from all investigated samples)

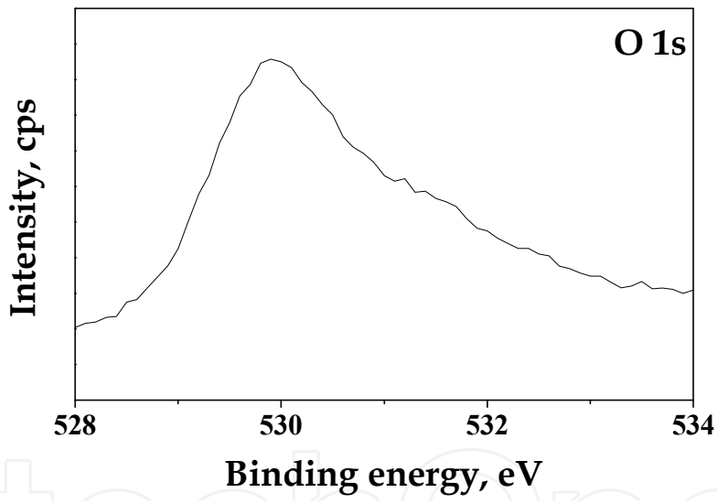

Fig. 13. XPS measurements for O1s from the CPs of the SGs (average results)

The XRD spectra obtained for different registered elements are presented with more details in the Figures 13 – 17. In general, these experimental results are in correlation with the Moessbauer investigations and also in fair agreement with the conclusions from the potentiodynamic polarization curves and SEM images. The presence of Cu is not a desired event since it could lead to local corrosion damages being more cathodic compared to iron.

As can be observed the main element with the highest content (in atomic percent) is oxygen followed by copper and iron as well as by much smaller amounts of Cr and Ni. In such a case it could be expected that the compounds on the surface will be mainly iron, copper or iron-copper oxides and hydroxides. The very low amounts of chromium and nickel compounds clearly demonstrate that their participation in the occurred corrosion processes is weaker expressed.

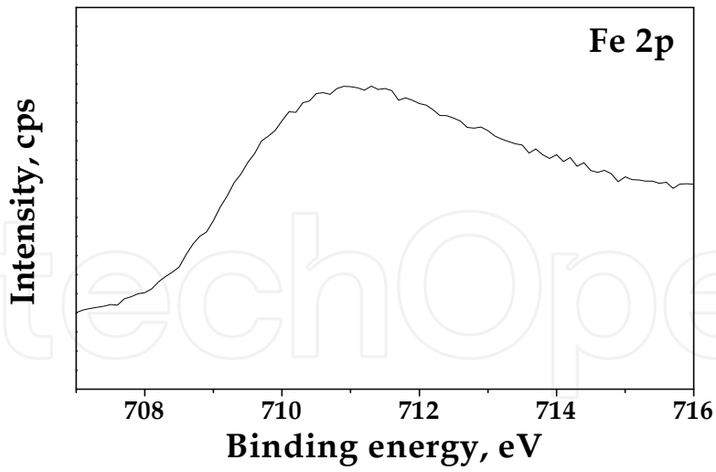

Fig. 14. XPS measurements for Fe2p from the CPs of the SGs (average results)

Element	Binding energy E, eV/ (at.%)	Possible compounds
O 1s	530,1 / (56,3) 531,6 / (37,0) 533,2 / (6,7)	Fe_2O_3; FeO; CuO FeOOH; $Cu(OH)_2$ H_2O
Cu 2p	932,8 / (57,0) 934,4 / (43,0)	Cu_2O; Cu. CuO; $Cu(OH)_2$; $CuCr_2O_4$

Table 4. Results after mathematical deconvolution of XPS investigations of CPs

However, the iron content is not very high which means that the used construction is to a definite degree protected at these conditions. The alloying elements nickel and chromium which are also registered during the investigations show practically their positive influence for the increased corrosion resistance of the used alloy.

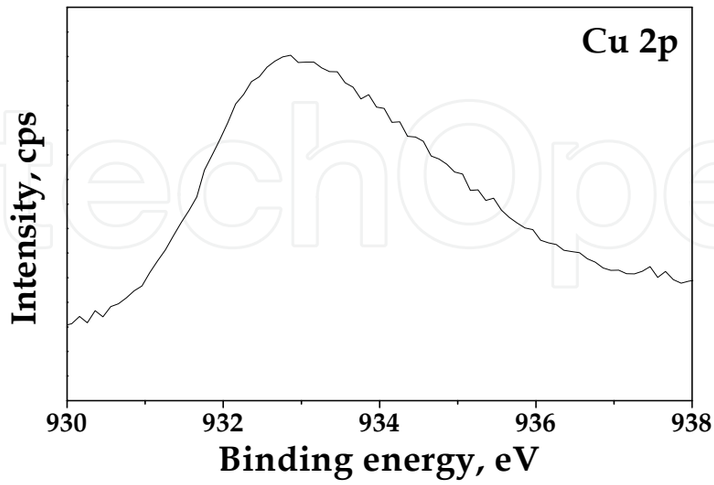

Fig. 15. XPS measurements for Cu2p from the CPs of the SGs (average results)

Aimed to receive clear results the XPS spectra obtained are additionally mathematically calculated using a special software aimed to determine also another peaks of possible

compounds that present in the sample but are not enough visible. This additional mathematical treatment known as "deconvolution process" gives more adequate information about the real situation in the samples. The results obtained are presented in Table 4 for two of the main elements – O1s and Cu2p.

The experimental data for the binding energy values of the main component presenting in the samples - oxygen – support the expectation that predominantly iron and copper oxides and hydroxides as well as water amounts appear - see Tables 3 and 4.

It follows from these data that the most possible iron compounds seems to be the oxides of Fe^{2+} and Fe^{3+} ions both latter presenting also in the composition of magnetite. This is a very important result as far as being in good correlation with the Moessbauer spectroscopy. Additionally, FeOOH has been detected but its amount seems to be lower compared to the quantities of bi- and trivalent iron oxides. The Cu spectrum demonstrates that this element has been detected mainly as pure metal and in its first oxidized state – in the form of Cu_2O and Cu. Their concentrations are comparable with the amounts of bivalent copper compounds – CuO, $Cu(OH)_2$ and most probably $CuCr_2O_4$.

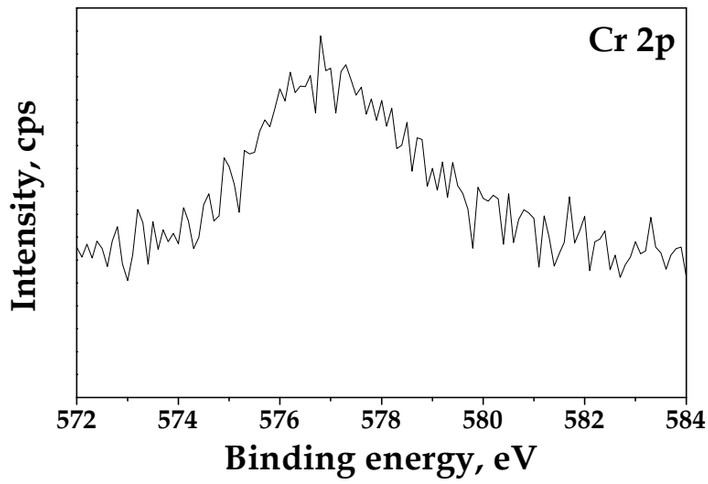

Fig. 16. XPS measurements for Cr2p from the CPs of the SGs (average results)

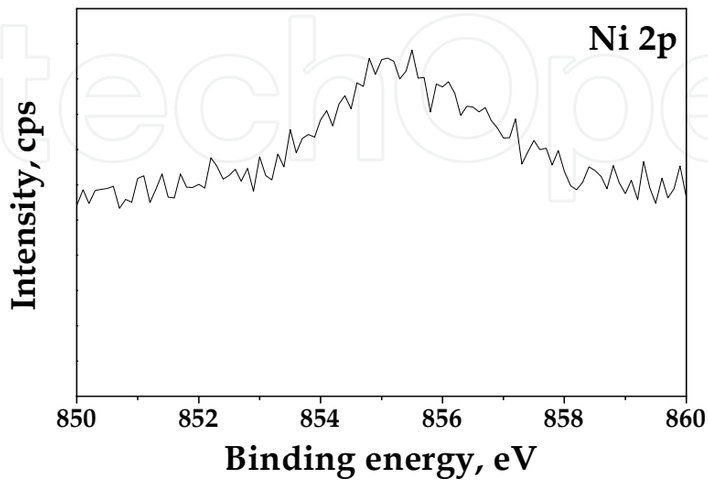

Fig. 17. XPS measurements for Ni2p from the CPs of the SGs (average results)

As already discussed above the other two elements (Ni and Cr) detected by XPS method are in much smaller amounts – about 1 at%. Nickel is in the form of Ni^{2+} ions, most probably as oxides and hydroxides - $NiO/Ni(OH)_2$. Chromium is registered in its third and sixth valencies (Cr_2O_3 and CrO_3) in a correlation between them of about 7:1. As can be registered these results differ to a certain degree with the results in Table 3 due to the mathematical treatment but from other side they confirm the general tendency of appearance of iron and copper hydroxides and other compounds. Main positive conclusion is that they are in agreement with the other used methods.

4. Conclusion

At model conditions and water chemistry regime applied, the corrosion current for austenitic stainless steel 18Cr10NiTi used in the construction is much lower compared to the low-alloyed steel. The investigations carried out at two operating temperatures and also at conditions close to the exploitation ones demonstrate the influence of selected corrosion activators on the most dangerous cases in the exploitation practice.

Having in mind the obtained results it can be concluded that the application of monoethanolamine significantly decrease the corrosion current density and leads to better corrosion resistance of the used steel. This compound also leads to appearing of middling slime with higher dispersion that can be easily removed from these places.

The corrosion processes occurring in the narrower cracks are more intensive compared to the processes in the wider cracks especially at higher temperatures and lead to faster destroying of the equipment at operating conditions. The application of MEA which is a "mixed" type inhibitor decrease partially the cathodic (oxygen reduction) and also the anodic (metal dissolution) reactions ensuring lower corrosion current density values and better protection against corrosion.

The presence of the protective layer of corrosion products of iron on the surface of the equipment is confirmed using Moessbauer spectroscopy and XPS investigations which are in fair agreement with the results obtained by the electrochemical polarization technique, SEM and EDX analysis. Taking into account that at real operation conditions in NPP "Kozloduy" and prolonged exploitation of the steam generators a film composed mainly of magnetite and hematite is readily formed on the pipe surfaces, it can be expected that the actual corrosion rate should be much lower.

Very important factor which influence the corrosion damages is the iron and copper concentration in the water of condense-feeding part of the SGs. This also affects their content in the corrosion products. Better exploitation conditions will be realized by periodical removing of the deposited corrosion products on the pipe bundles and on the other places in the steam generators where they appear.

5. References

Andreeva M. et. al., (2008). Overview of plant specific severe accident management strategies for Kozloduy nuclear power plant, WWER-1000/320, *Annals of Nuclear Energy*, v. 35, pp. 555–564, ISSN: 0306-4549.

R.W. Staehle and J.A. Gorman, (2003), Quantitative Assessment of Submodes of Stress Corrosion Cracking on the Secondary Side of Steam Generator Tubing in PWRs;

Part I, II & III, *Corrosion,* v. 59, No. 11, pp. 931-994; Houston, TX: NACE, ISSN 0010-9312

R.W. Staehle and J.A. Gorman, (2004), Quantitative Assessment of Submodes of Stress Corrosion Cracking on the Secondary Side of Steam Generator Tubing in PWRs; Part I, II & III, *Corrosion,* v. 60, No. 1, pp. 5-63; Houston, TX: NACE, ISSN 0010-9312

R.W. Staehle and J.A. Gorman, (2004), Quantitative Assessment of Submodes of Stress Corrosion Cracking on the Secondary Side of Steam Generator Tubing in PWRs; Part I, II & III, *Corrosion,* v. 60, No. 2, pp. 115-180; Houston, TX: NACE, ISSN 0010-9312

J. Congleton, T. Shoji and R.N. Parkins, (1985), "The Stress Corrosion Cracking of Reactor Pressure Vessel Steel in High-Temperature Water, *Corrosion Science*, v. 25, No. 8/9, p. 633-650, ISSN: 0010-938X .

Sviridenko, I., (2008). Heat exchangers based on low temperature heat pipes for autonomous emergency WWER cooldown systems, *Applied Thermal Engineering*, v. 28, pp. 327 – 324, ISSN: 1359-4311

Hadavi, S.M.H., (2008). WWER-1000 shutdown probabilistic risk assessment: An introductory insight, *Annals of Nuclear Energy,* v. 35, pp. 196-206, ISSN: 0306-4549

Viehrig, H.-W., et. al., (2006). Application of advanced master curve approaches on WWER-440 reactor pressure vessel steels, *International Journal of Pressure Vessels and Piping*, v. 83, pp. 584–592, ISSN: 0308-0161

Slugen, V., et. al., (2005). Corrosion of steam generator pipelines analysed using Moessbayer spectroscopy, *Nuclear Engineering and Design*, v. 235, pp. 1969–1976, ISSN: 0029-5493

Raichevski G. et al., Corrosion investigations and SEM studies of austenitic stainless steel used in the steam generators of the Nuclear Power Plant "Kozloduy", First International Conference "Corrosion and Material Protection", EFC event No. 294, paper No. 72, ISBN 978-80-903933-0-1, Prague, Czech Republic, 01 – 04 October 2007.

Hojna A. et. al, Electrochemical evaluation system – modular system for long-term on-line monitoring of corrosion processes in structural crevices of steam generator secondary circuits, First International Conference "Corrosion and Material Protection", EFC event No. 294, paper No. 83, ISBN 978-80-903933-0-1, Prague, Czech Republic, 01 – 04 October 2007.

Kaczorowski D. et. al., (2006). Water chemistry effect on the wear of stainless steel in nuclear power plant, *Tribology International*, v. 39, pp. 1503 – 1508, ISSN: 0301-679X.

Zubchenko, A.S., et. al., (2004). Effect of nickel content on mechanical properties and fracture toughness of weld metal of WWER-1000 reactor vessel welded joints, *International Journal of Pressure Vessels and Piping*, v. 81, pp. 713 – 717, ISSN: 0308-0161

Slugen, V., et. al., (2002). Moessbauer spectroscopy used for testing of reactor steels, *NDT&E International* (*Independent Nondestructive Testing and Evaluation*), v. 35, pp. 511 – 518, ISSN: 0963-8695

Lunin, G.L., et. al., (1997)., Status and further development of nuclear power plants with WWER in Russia, *Nuclear Engineering and Design*, v. 173, pp. 43 – 57 , ISSN: 0029-5493

N.D. Budiansky, et al., (2005), Detection of Interactions Among Localized Pitting Sites on Stainless Steel Using Spatial Statistics, *Journal of the Electrochemical Society*, v.152, No. 4, pp. B152-B160, ISSN: 0013-4651.

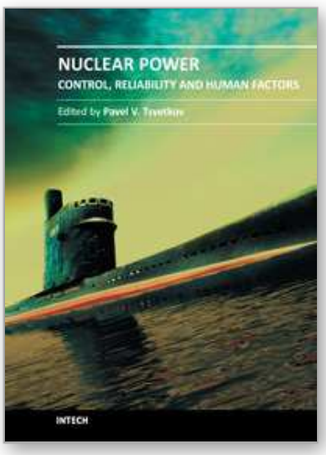

Nuclear Power - Control, Reliability and Human Factors
Edited by Dr. Pavel Tsvetkov

ISBN 978-953-307-599-0
Hard cover, 428 pages
Publisher InTech
Published online 26, September, 2011
Published in print edition September, 2011

Advances in reactor designs, materials and human-machine interfaces guarantee safety and reliability of emerging reactor technologies, eliminating possibilities for high-consequence human errors as those which have occurred in the past. New instrumentation and control technologies based in digital systems, novel sensors and measurement approaches facilitate safety, reliability and economic competitiveness of nuclear power options. Autonomous operation scenarios are becoming increasingly popular to consider for small modular systems. This book belongs to a series of books on nuclear power published by InTech. It consists of four major sections and contains twenty-one chapters on topics from key subject areas pertinent to instrumentation and control, operation reliability, system aging and human-machine interfaces. The book targets a broad potential readership group - students, researchers and specialists in the field - who are interested in learning about nuclear power.

InTech Europe
University Campus STeP Ri
Slavka Krautzeka 83/A
51000 Rijeka, Croatia
Phone: +385 (51) 770 447
Fax: +385 (51) 686 166
www.intechopen.com

InTech China
Unit 405, Office Block, Hotel Equatorial Shanghai
No.65, Yan An Road (West), Shanghai, 200040, China
中国上海市延安西路65号上海国际贵都大饭店办公楼405单元
Phone: +86-21-62489820
Fax: +86-21-62489821

IntechOpen